*chemosensors*

MDPI

*Article*

# Fast Determination and Source Apportionment of Eight Polycyclic Aromatic Hydrocarbons in PM10 Using the Chemometric-Assisted HPLC-DAD Method

**Ting Hu †, Yitao Xia †, You Wang, Li Lin, Rong An, Ling Xu and Xiangdong Qing ***

Hunan Provincial Key Laboratory of Dark Tea and Jin-hua, College of Materials and Chemical Engineering, Hunan City University, Yiyang 413000, China; 18773784330@163.com (T.H.); 13627378597@163.com (Y.X.); wy15080709653@163.com (Y.W.); linli@hncu.edu.cn (L.L.); anrong@hncu.edu.cn (R.A.); xuling@hncu.edu.cn (L.X.)

* Correspondence: xdqing123@hnu.edu.cn

† These authors contributed equally to this work.

**Abstract:** Polycyclic aromatic hydrocarbons (PAHs) are a group of organic compounds that are both toxic and hazardous to human health and ecological systems. In recent work, a novel analytical strategy based on the chemometric-assisted HPLC-DAD method was proposed for the quantification and source apportionment of eight PAHs in PM10 samples. Compared to traditional chromatographic methods, this approach does not require the purification of complex PM10 samples. Instead, it utilizes a mathematical separation method to extract analytes' profiles from overlapping chromatographic peaks, enabling precise quantification of PAHs in PM10. Firstly, 40 PM10 samples collected in Loudi city during two sampling periods were used for analysis. Subsequently, the second-order calibration method based on alternating trilinear decomposition (ATLD) was employed to handle the three-way HPLC-DAD data. Finally, the pollution sources of PAHs were analyzed by the feature component analysis method according to the obtained relative concentration matrix. For the validation model, the average recoveries of eight PAHs were between (88.8 ± 7.6)% and (105.6 ± 7.5)%, and the root-mean-square errors of prediction ranged from 0.03 μg $mL^{-1}$ to 0.47 μg $mL^{-1}$. The obtained limits of quantification for eight PAHs were in the range of 0.0050 μg $mL^{-1}$ to 0.079 μg $mL^{-1}$. For actual PM10 samples, results of the feature component analysis indicated that the main source of PAHs in PM10 may be traffic emissions and coal combustion. In summary, the proposed method provided a new and rapid analysis method for the accurate determination and source apportionment of PAHs in atmospheric aerosols.

**Keywords:** PAHs; PM10; HPLC-DAD; ATLD; source apportionment

check for updates

**Citation:** Hu, T.; Xia, Y.; Wang, Y.; Lin, L.; An, R.; Xu, L.; Qing, X. Fast Determination and Source Apportionment of Eight Polycyclic Aromatic Hydrocarbons in PM10 Using the Chemometric-Assisted HPLC-DAD Method. *Chemosensors* **2024**, *12*, 220. https://doi.org/10.3390/chemosensors12100220

Received: 21 August 2024
Revised: 10 October 2024
Accepted: 15 October 2024
Published: 18 October 2024

**Copyright:** © 2024 by the authors. Licensee MDPI, Basel, Switzerland. This article is an open access article distributed under the terms and conditions of the Creative Commons Attribution (CC BY) license (https://creativecommons.org/licenses/by/4.0/).

## 1. Introduction

Polycyclic aromatic hydrocarbons (PAHs) are composed of two or more fused benzene rings arranged in various structural configurations. They have attracted significant attention from researchers in the environmental field, due to their carcinogenic, persistent, and mutagenic characteristics [1]. PAHs can be found in the environment from both natural sources such as biosynthesis, volcanic eruptions, and forest fires, as well as anthropogenic activities such as fossil fuel combustion, industrial processes, and vehicle emissions [2–6]. Gaseous and solid states are their primary forms of existence in the atmosphere. Most PAHs are adsorbed onto the surface of atmospheric particulate matter, primarily on fine inhalable particles, which can be directly inhaled into the lungs, leading to respiratory and cardiovascular diseases and posing significant health risks to humans [2,7–9]. Therefore, the fast determination and source apportionment of PAHs in atmospheric particulate matter can provide a theoretical basis for effectively controlling PAH pollution, benefiting both environmental protection and human health.

High-performance liquid chromatography with a diode array detector (HPLC-DAD) is widely used in the analysis of PAHs in the environment, food, biological matrices, and so on [10–14]. Different from the UV-vis detection-HPLC, HPLC-DAD produces an elution time-spectral second-order data matrix through each run. A three-way data array is obtained with different chromatographic runs, in which the third dimension is the number of samples. Rich qualitative and quantitative information of analytes can be extracted from the generated three-way data array. By adding an additional dimension such as pH, reaction time, or reaction temperature, higher-dimensional data can be produced from a set of samples [15–17]. Therefore, it has long been a significant challenge to effectively and rapidly analyze these high-dimensional data in chromatographic analysis. Additionally, there are other commonly occurring issues such as baseline drifts, peaks co-eluting, retention-time shifts, matrix effect, and so on, which present challenges for the analysis of complex actual samples with HPLC-DAD [18,19].

Fortunately, chemometric second-order calibration methods provide an effective solution to these challenges. They enable rapid and accurate identification and quantification of target analytes even in the presence of uncalibrated or unknown interferences, which is known as "second-order advantage" [15,19,20]. Currently, there are some widely used algorithms contributing to second-order data analysis, including parallel factor analysis (PARAFAC) [21], multivariate curve resolution-alternating least squares (MCR-ALS) [22], alternating trilinear decomposition (ATLD) [23,24], alternating penalty trilinear decomposition (APTLD) [25], and self-weighted alternating trilinear decomposition (SWATLD) [26]. They have been widely applied in various fields. For example, the ATLD algorithm was utilized by Zhang et al. to mathematically decompose the three-dimensional data array of HPLC-DAD for quantitative analysis of seven flavonoids in honey [27]. PARAFAC and GC-MS were employed by Valverde-Som et al. to conduct qualitative and quantitative analyses of polymer additive residues in coffee [28]. Three-dimensional fluorescence coupled with second-order calibration was applied to quantitatively analyze residues of cypermethrin and thiodicarb in food [29]. These research results demonstrated the excellent performance of second-order calibration methods, e.g., avoiding the tedious sample pretreatment process, overcoming baseline drift, and addressing slight retention-time shifts and peak overlap in the chromatographic analysis.

In recent work, a simple and green analytical strategy that combined the second-order calibration based on the alternating trilinear decomposition algorithm (ATLD) with HPLC-DAD was proposed for the accurate determination of eight PAHs in PM10 samples. Based on the obtained concentrations of eight PAHs in PM10, the feature component analysis method was used to source-apportion PAHs in PM10. In addition, a simple preprocessing procedure based on ultrasonic-assisted extraction and solvent evaporation under reduced pressure was applied to extract and concentrate PAHs from PM10 samples. Moreover, the problems of baseline drift and peak overlap were also addressed with the proposed method in the work.

## 2. Experiment

### *2.1. Reagents and Chemicals*

The eight PAHs included acenaphthylene (ACN, analytical standard), fluorene (FLU, ≥99.5%), phenanthrene (PHE, analytical standard, ≥99%), anthracene (ANT, ≥99.5%), pyrene (PYR, analytical standard), benzo[α]-anthracene (BaA, analytical standard), chrysene (CHR, ≥97%), and naphthalene (NAP, ≥99.7%), which were supplied by Aladdin Biochemical Technology Co., Ltd. (Shanghai, China). Methanol (HPLC grade, 99.9%) was also obtained from Aladdin Biochemical Technology Co., Ltd. Other solvents, including dichloromethane (Analytical reagent (AR), ≥99.5%) and n-hexane (AR, ≥97.0%), were sourced from Hunan Hui-hong Reagent Co., Ltd. (Changsha, China).

### *2.2. Instrumentation*

Retention time-spectral wavelength matrices were produced using HPLC (Shimadzu Corporation, Kyoto, Japan), which consisted of a degasser, two pumps (LC-20AD), an

auto-injector (SIL-20A), a column oven (CTO-20A), and a diode array detector (DAD, SPD-M20A) featuring both deuterium and tungsten lamps. Separation was performed using an analytical reversed-phase column InertSustain®-C18 (5.0 µm, 4.6 mm × 250 mm) purchased from Shimadzu, Japan. The extraction of PAHs was carried out using an ultrasonic instrument (KQ-00E) from Kunshan Shumei Ultrasonic Instrument Co., Ltd. (Kunshan, China). The PM10 samples were collected by a high-capacity air sampler (JH-2020) produced by Qingdao Jinghong Environmental Protection Technology Company (Qingdao, China). The rotary evaporator (RE-201D) was manufactured by Laica Instruments Ltd. The desktop high-speed centrifuge (LC-LX-H165A) was provided by Shanghai Yichen Bangxi Instrument Technology Co., Ltd. (Shanghai, China).

Methanol–water was selected as the mobile phase of HPLC at a flow rate of 1.0 mL $min^{-1}$. The DAD detection wavelength was set between 190 and 800 nm with a spectral resolution of 1.2 nm. The sample injection volume was 20 µL.

### *2.3. Standard Solutions*

The standard solutions of eight PAHs were prepared by dissolving appropriate weights of each standard substance in methanol. The concentrations of the eight stock solutions were 20.0, 119.0, 7.8, 98.0, 56.0, 64.0, 6.8, and 50.0 µg $mL^{-1}$ for CHR, ACN, FLU, PHE, ANT, PYR, BaA, and NAP, respectively. To prevent the PAHs from volatilizing and degrading due to light exposure, the stock solutions were stored at −4 °C, protected from light.

### *2.4. Sampling Procedure*

Four high-capacity air samplers were used to simultaneously collect PM10 samples at four locations in Loudi City, China, including the Lian-Gang steel industry (LG1-LG5), the municipal government (MG1-MG5), the municipal monitoring station (MS1-MS5), and the municipal party school (MP1-MP5). The sampling time for each sample was 24 h, and the collected PM10 samples were adsorbed on quartz fiber filter membranes with a diameter of 80 mm (Qingdao Jinghong Environmental Protection Technology Company). The four sampling locations are shown in Figure 1. Five PM10 samples were collected at each location during a sampling period. Forty PM10 samples were collected in two different seasons, including Spring and Winter, as PM10 sample set 1 and sample set 2, respectively. The weight of these prepared samples was accurately measured, and they were stored in pre-drying bags at suitable temperature conditions (−20 °C) for further analysis.


**Figure 1.** Distribution of atmospheric particulate matter sampling locations.

### *2.5. PAH Extraction*

Ultrasonic extraction and solvent evaporation under reduced pressure were used to extract and concentrate PAHs to meet the analytical requirements for PAH traces in PM10. Firstly, the accurately weighed sample of filter membrane (around 0.44 g) was cut into pieces and transferred into a 20.0 mL centrifuge tube, followed by the addition of 4.0 mL dichloromethane and 6.0 mL n-hexane as the solvent for ultrasonic extraction for 15 min at room temperature. Then, the mixture was filtered, and the filtrate was collected. Next, 2.0 mL of mobile phase solution was added to the filtrate, and the mixed solution was concentrated to approximately 2.0 mL by a rotary evaporator in a 60 °C water bath, and the solution was transferred to a 5.0 mL centrifuge tube and centrifuged at 15,000 r/min for 5 min to remove suspended matter. Finally, the supernatant was put into a 2.0 mL sample vial with a sealing plastic wrap and refrigerated at −4 °C until analysis.

### *2.6. Sample Sets*

According to the concentrations' design in Table 1, seven calibration samples were prepared by mixing appropriate volumes of each PAH stock solution and diluting them with pure methanol into 10.0 mL brown volumetric flasks. Subsequently, six validation samples were prepared in the same way as the calibration samples, and these were used to verify the reliability of the ATLD method. The concentrations of eight PAHs in the validation samples were randomly selected in the range of 0.06 to 6.70 μg·mL$^{-1}$, as shown in Table 1. Although the concentrations of PAHs in the validation samples differed from those in the calibration samples, they were all within the concentration range of calibration samples. Prior to HPLC-DAD analysis, all samples were filtered using a 0.22 μm non-sterile PTFE syringe filter (i-Quip® N2536). The measured samples by HPLC-DAD included 40 PM10 samples, 7 calibration samples, and 6 validation samples.

**Table 1.** Concentrations of eight PAHs in seven calibration samples (C01–C07) and six validation samples (V01–V06), respectively.

| Sample No. | Analyte Concentration (μg·mL$^{-1}$) | | | | | | | |
|---|---|---|---|---|---|---|---|---|
| | **CHR** | **NAP** | **ACN** | **FLU** | **PHE** | **ANT** | **PYR** | **BaA** |
| C01 | 0.30 | 0.00 | 0.00 | 0.39 | 0.00 | 0.00 | 0.00 | 0.00 |
| C02 | 0.00 | 5.00 | 0.00 | 0.00 | 4.41 | 0.00 | 6.40 | 0.00 |
| C03 | 0.00 | 0.00 | 6.70 | 0.00 | 0.00 | 5.60 | 0.00 | 0.68 |
| C04 | 0.24 | 2.50 | 1.34 | 0.31 | 0.98 | 3.36 | 5.12 | 0.34 |
| C05 | 0.18 | 3.50 | 5.36 | 0.23 | 4.16 | 4.48 | 1.28 | 0.48 |
| C06 | 0.12 | 4.00 | 2.68 | 0.16 | 1.96 | 1.12 | 3.84 | 0.54 |
| C07 | 0.06 | 4.50 | 4.02 | 0.08 | 2.45 | 2.24 | 2.56 | 0.61 |
| V01 | 0.30 | 2.50 | 2.01 | 0.39 | 0.98 | 1.96 | 5.76 | 0.32 |
| V02 | 0.24 | 2.18 | 2.68 | 0.31 | 1.47 | 3.08 | 5.12 | 0.41 |
| V03 | 0.18 | 3.25 | 3.35 | 0.27 | 1.96 | 5.32 | 4.48 | 0.65 |
| V04 | 0.15 | 4.75 | 4.08 | 0.23 | 2.45 | 4.76 | 1.92 | 0.58 |
| V05 | 0.12 | 4.25 | 5.36 | 0.20 | 3.43 | 4.20 | 3.20 | 0.51 |
| V06 | 0.09 | 3.75 | 6.03 | 0.16 | 3.92 | 3.64 | 3.84 | 0.44 |

## 3. Method and Software

In the study, alternating trilinear decomposition (ATLD) was employed to analyze the three-dimensional data array of PM10 samples. This method was originally introduced by Wu et al. in 1998 [23]. It adopts the principle of alternating least squares and introduces the Moore–Penrose generalized inverse calculation based on singular value decomposition (SVD). This, combined with alternating iteration steps, improves the performance of trilinear decomposition by minimizing the sum of squared elements in the loss function or residual matrix. ATLD is renowned for its rapid convergence and resilience to the presence of excessive factors, making it a highly suitable tool for decomposing three-way data in

complex environmental scenarios. Detailed discussions on the principles and applications of ATLD can be accessed in the relevant literature [23].

Feature component analysis was used to classify PM10 samples collected from four locations and two sampling seasons, which was done on the Systat SigmaPlot software (Version 13.0, www.systatsoftware.com (accessed on 16 October 2024)). The data analysis process was performed on a computer running Windows 11, and the acquired data were processed using MATLAB (Version R2015b, MathWorks Inc., Natick, MA, USA) software.

## 4. Results and Discussions

### *4.1. Optimization of HPLC Conditions*

Before analysis, the mobile phase with different ratios of methanol–water (100:0, 90:10, and 80:20) was initially investigated. The 90:10 methanol–water mixture was selected for its ability to achieve the most selective detection of PAHs. Subsequently, the effects of linear ranges of analyte concentrations and temperature on the chromatographic peak shape of analytes were explored. By regressing the chromatographic peak area and concentrations of PAHs, the linear ranges of the eight analytes were established as follows: 1.12–56.00 μg $mL^{-1}$ for ANT, 0.08–7.80 μg $mL^{-1}$ for FLU, 0.32–6.80 μg $mL^{-1}$ for BaA, 0.98–98.00 μg $mL^{-1}$ for PHE, 1.34–119.00 μg $mL^{-1}$ for ACN, 0.06–20.00 μg $mL^{-1}$ for CHR, 1.28–64.00 μg $mL^{-1}$ for PYR, and 2.18–50.00 μg $mL^{-1}$ for NAP. Additionally, in order to test the influence of temperature on the peak shape of analytes, the column temperature conditions of 30, 35, and 40 °C were also investigated. It was found that when the column temperature of 40 °C was selected, the phenomenon of peak dragging was avoided, especially for ANT, PYR, and ACN. To ensure the validity of this method, all analyte concentrations in the experiment were measured within the linear ranges established and at a column temperature of 40 °C.

### *4.2. Model Validation*

Seven calibration samples and six validation samples, as a validation model, were subjected to HPLC-DAD analysis, and a three-dimensional data array was generated. Then, the ATLD algorithm was used to decompose the data array, and the quantitative and statistical results for the eight PAHs in the validation samples are shown in Table 2.

**Table 2.** Quantitative and statistical results of ATLD analysis of eight PAHs in validation samples.

| Sample | Predicted Concentration (μg $mL^{-1}$) [Recovery (%)] | | | | | | | |
|---|---|---|---|---|---|---|---|---|
| | **CHR** | **NAP** | **ACN** | **FLU** | **PHE** | **ANT** | **PYR** | **BaA** |
| V01 | 0.35 [114.3] | 2.42 [92.6] | 2.01 [98.4] | 0.39 [99.3] | 0.98 [90.7] | 1.75 [87.4] | 6.03 [105.6] | 0.36 [113.6] |
| V02 | 0.27 [113.4] | 2.63 [116.1] | 2.68 [99.3] | 0.3 [96.1] | 1.39 [88.8] | 3.22 [104.1] | 5.2 [102.1] | 0.38 [95.2] |
| V03 | 0.19 [108.1] | 2.96 [88.9] | 3.32 [98.5] | 0.24 [87.8] | 1.8 [88.4] | 5.59 105.5] | 4.24 [94.3] | 0.6 [92.0] |
| V04 | 0.17 [111.2] | 4.55 [96.4] | 4.06 [99.2] | 0.21 [92.0] | 2.36 [94.9] | 4.98 [105.0] | 1.69 [82.2] | 0.51 [88.6] |
| V05 | 0.11 [93.4] | 3.53 [82.2] | 5.12 [95.6] | 0.15 [75.0] | 2.91 [84.3] | 4.14 [98.6] | 2.67 [80.9] | 0.43 [85.2] |
| V06 | 0.08 [97.5] | 3.24 [84.9] | 5.87 [97.6] | 0.13 [79.3] | 3.44 [87.9] | 3.68 [100.9] | 3.22 [82.5] | 0.36 [81.9] |
| AR [a] | 105.6 | 95.7 | 98.6 | 88.8 | 92.6 | 100.6 | 92.7 | 92 |
| AD [b] | 7.5 | 9.2 | 0.9 | 7.6 | 4.2 | 4.7 | 9.4 | 7.5 |
| RMSEP [c] | 0.03 | 0.47 | 0.13 | 0.03 | 0.33 | 0.19 | 0.41 | 0.07 |
| RRMSEP [d] | 15.4 | 13.6 | 3.3 | 11. 6 | 13.9 | 5.1 | 10.2 | 13.9 |
| *t*-test [e] | 1.22 | 0.73 | 1.84 | 2.86 | 2.89 | 0.21 | 1.79 | 1.65 |
| $R^2$ [f] | 0.9399 | 0.9995 | 0.9997 | 0.9962 | 0.9988 | 0.9995 | 0.9922 | 0.9999 |
| SEN [g] | 4.66 | 1.08 | 2.87 | 34.69 | 1.16 | 4.44 | 2.26 | 7.96 |

**Table 2.** *Cont.*

| Sample | Predicted Concentration (μg mL$^{-1}$) [Recovery (%)] | | | | | | | |
|---|---|---|---|---|---|---|---|---|
| | **CHR** | **NAP** | **ACN** | **FLU** | **PHE** | **ANT** | **PYR** | **BaA** |
| SEL [h] | 0.07 | 0.32 | 0.17 | 0.36 | 0.05 | 0.14 | 0.16 | 0.31 |
| LOD [i] | 0.0062 | 0.016 | 0.012 | 0.0043 | 0.026 | 0.076 | 0.023 | 0.0016 |
| LOQ [i] | 0.019 | 0.048 | 0.036 | 0.013 | 0.079 | 0.23 | 0.07 | 0.005 |

[a] AR, average recovery, %. [b] AD, average deviation, %. [c] The root mean square error of prediction (RMSEP, μg mL$^{-1}$) can be calculated as follows: RMSEP $= \left[\frac{1}{I-1}\sum\left(c_{act}-c_{pred}\right)^2\right]^{1/2}$. [d] The relative root mean square error of prediction (RRMSEP, %) can be calculated as follows: RRMSEP $= \left[\frac{1}{I-1}\sum\left(c_{act}-c_{pred}\right)^2\right]^{1/2}/\overline{x}\times 100\%$, where $c_{act}$ and $c_{pred}$ are the actual and predicted concentration, respectively. I is the number of prediction samples. $\overline{x}$ is the average concentration in prediction samples. [e] $T = (\overline{X}-\mu_0)/(S/\sqrt{n})$, where $\overline{x}$ is the average recovery, $\mu_0$ is 100%, n is the degree of freedom (where n + 1 is the number of evaluated levels), and confidence level is 95%; here, $T^5_{0.025}$= 2.57. [f] Correlative coefficient ($R^2$). [g] $SEN_{FO3} = s_n\left\{\left[\left(\mathbf{A}_{cal}{}^T\mathbf{P}_{A,unx}\mathbf{A}_{cal}\right)*\left(\mathbf{B}_{cal}{}^T\mathbf{P}_{B,unx}\mathbf{B}_{cal}\right)\right]^{-1}\right\}^{-1/2}_{nn}$. [h] SEL =SEN/$s_n$. [i] LOD (limit of detection, μg mL$^{-1}$) is calculated by LOD = 3.3$\sigma_0$; LOQ (limit of quantification, μg mL$^{-1}$) is estimated with LOQ = 10$\sigma_0$, where $\sigma_0$ is the standard deviation in predicted concentrations of analytes of interest in three blank samples.

Several key statistical parameters such as root mean square error of prediction (RMSEP), *t*-test, and correlation coefficient ($R^2$), as well as figures of merit including limit of detection (LOD), limit of quantification (LOQ), sensitivity (SEN), and selectivity (SEL), were computed to assess the accuracy of the method. From the table, it could be observed that the ATLD algorithm exhibited a good predictive capability for the eight PAHs in the validation samples, with RMSEP values below 0.47 μg mL$^{-1}$ and RRMSEP values below 15.4%. The average recoveries of the eight PAHs ranged from 88.8% to 105.6%, with average deviations below 9.4%. *t*-test values are below the reference value of 2.57, except for FLU and PHE, indicating that there were no significant differences in the prediction of PAH concentrations in the validation samples. These results demonstrated that the proposed method was accurate and reliable for detecting PAHs in the validation samples. Therefore, the developed method will be applied to analyze complex PM10 samples in the following section.

### *4.3. Quantification of PAHs in PM10 Samples*

Figure 2 provides the molecular structures of the eight PAHs. The chromatograms of 7 calibration samples, 6 validation samples, 1 blank sample, and 40 PM10 samples are displayed in Figure 3. From Figure 3, it can be observed that under the optimal HPLC-DAD conditions, all eight PAHs were completely eluted within 13 min. However, it was evident that there exhibited issues of severe peak overlap, baseline drift, and slight retention-time shift across all samples. In such a complex practical system, it was challenging to accurately identify and quantify PAHs using traditional chromatographic methods and univariate calibration.

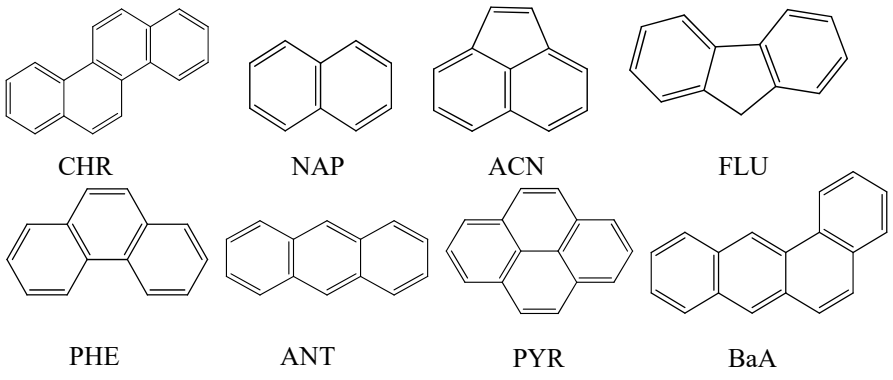


**Figure 2.** Molecular structures of the eight PAHs.

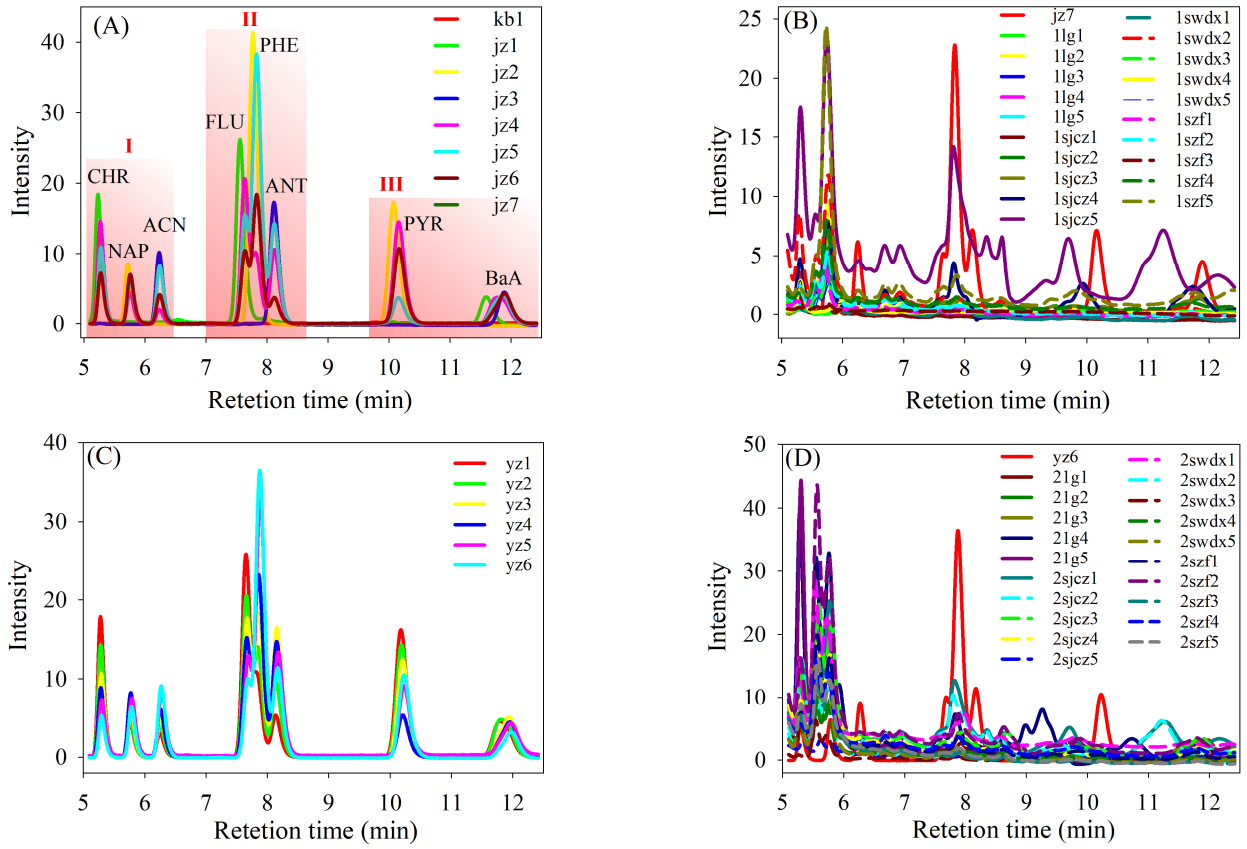


**Figure 3.** Chromatograms of all samples. (**A**) Seven calibration samples and one blank sample; (**B**) PM10 samples in sample set 1; (**C**) six validation samples; (**D**) PM10 samples in sample set 2.

In response to the aforementioned issues, the second-order calibration method utilized "mathematical separation" instead of "chemical or physical separation", enabling the extraction of effective information of target analytes from HPLC-DAD data of complex systems, thereby improving the accuracy and reliability of the analysis method. Before applying the ATLD approach, the elution regions of eight PAHs were divided into three sub-segments, including 5.10~6.65 min (I), 7.23~8.67 min (II), and 9.71~12.42 min (III) (Figure 3A), which were based on spectral features and corresponding elution times for the effective analysis of each analyte. Subsequently, the number of chemical components (*N*) in each sub-segment was estimated by the core consistency diagnostic method [30]. The *N* values of the three subregions (I, II, and III) were 10, 8, and 6, respectively. Following this, three three-dimensional data arrays containing 7 calibration samples, 6 validation samples, and 40 PM10 samples were established for ATLD analysis. These multicomponent models were resolved by ATLD with the suggested N values. Then, the resolved chromatographic and spectral profiles for each PAH were compared with their actual profiles in the calibration samples, which served as a qualitative basis for the rapid identification of PAHs of interest in PM10.

Figure 4 presents the chromatographic, spectral, and relative concentration profiles of the eight PAHs in 7 calibration samples and 40 PM10 samples. As shown in Figure 4A1–A3, the baseline drift was successfully eliminated as an additional factor. Among them, ANT, FLU, and PHE eluted very close to each other and seriously overlapped within 1.40 min. This is because their molecular structures are very similar, even when they are isomers such as PHE and ANT. Additionally, the issue of slight retention-time shifts, especially for PYR and BaA, was also successfully addressed with the proposed method.

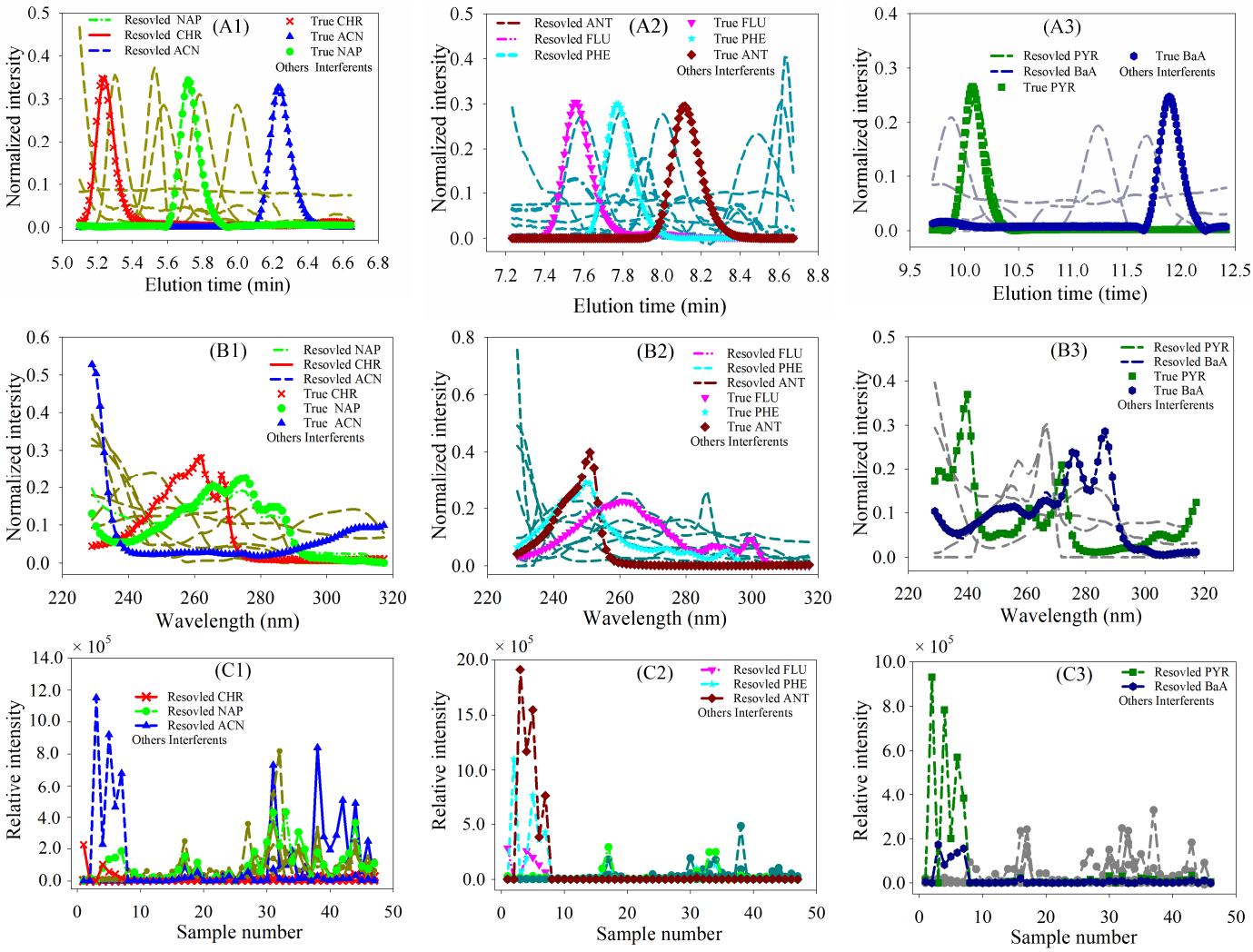


**Figure 4.** A pictorial display of the resolved results of the eight PAHs in 7 calibration samples and 40 PM10 samples by ATLD. (**A1**–**A3**), normalized elution time profiles; (**B1**–**B3**), normalized spectra profiles; (**C1**–**C3**), relative concentration profiles.

The similarity in the PAHs' structures led to similar interactions on the C18 reversed-phase analytical column, which ultimately resulted in the severe co-elution issue. However, ATLD effectively returned clear chromatographic and spectral profiles for each analyte, with the resolved profiles closely aligning with their references. The satisfactory results confirmed that the ATLD method effectively addressed the problems of baseline drift, peak overlap, and slight retention-time shift in this case. The strategy based on the second-order calibration combined with HPLC-DAD avoided the time-consuming pretreatment steps and addressed the issues of peak overlap and slight retention-time shifts of targeted analytes of interest with interfering substances, thus successfully obtaining accurate qualitative results of the eight PAHs in PM10 samples.

The predicted concentrations of PAHs in sample set 1 and sample set 2 are listed in Tables 3 and 4, respectively. It was found that the total concentrations of PAHs in PM10 samples for sample sets 1 and 2 ranged from 0.046 $\mu g \cdot mL^{-1}$ to 3.70 $\mu g \cdot mL^{-1}$ and from 0.33 $\mu g \cdot mL^{-1}$ to 8.75 $\mu g \cdot mL^{-1}$, respectively. Among these, the concentrations of NAP, ACN, PHE, and BaA were the highest in all samples from the four locations. Additionally, the concentration levels of PAHs differed across various sampling periods and locations, likely due to changes in pollution sources and environmental conditions.

**Table 3.** The predicted concentrations of PAHs in PM10 in sample set 1.

| Samples | Predicted Values (μg mL$^{-1}$) | | | | | | | | |
|---|---|---|---|---|---|---|---|---|---|
| | **CHR** | **NAP** | **ACN** | **FLU** | **PHE** | **ANT** | **PYR** | **BaA** | **∑PAHs** |
| LG1 [b] | ND [a] | 0.069 | ND | ND | ND | ND | ND | ND | 0.069 |
| LG2 [b] | ND | 0.96 | 0.072 | ND | ND | ND | ND | ND | 1.03 |
| LG3 [b] | ND | 0.36 | ND | ND | ND | ND | ND | ND | 0.36 |
| LG4 [b] | ND | 0.096 | ND | ND | ND | ND | ND | ND | 0.096 |
| LG5 [b] | ND | 0.41 | ND | ND | ND | ND | ND | ND | 0.41 |
| MS1 [c] | ND | 0.080 | ND | ND | ND | ND | ND | ND | 0.080 |
| MS2 [c] | ND | 0.30 | ND | ND | ND | ND | ND | ND | 0.30 |
| MS3 [c] | ND | 0.45 | 0.077 | ND | ND | ND | ND | ND | 0.53 |
| MS4 [c] | ND | 1.23 | 0.13 | ND | 0.33 | ND | ND | 0.064 | 1.75 |
| MS5 [c] | ND | 2.70 | 0.22 | 0.020 | 0.76 | ND | ND | ND | 3.70 |
| MG1 [d] | ND | 0.20 | 0.24 | ND | ND | ND | ND | ND | 0.44 |
| MG2 [d] | ND | 2.02 | 0.58 | ND | 0.079 | ND | ND | ND | 2.68 |
| MG3 [d] | ND | 0.11 | 0.037 | ND | ND | ND | ND | ND | 0.15 |
| MG4 [d] | ND | 0.078 | ND | ND | ND | ND | ND | ND | 0.078 |
| MG5 [d] | ND | 0.44 | 0.061 | ND | ND | ND | ND | ND | 0.50 |
| MP1 [e] | ND | 0.060 | 0.068 | ND | ND | ND | ND | ND | 0.13 |
| MP2 [e] | ND | 0.77 | 0.34 | ND | ND | ND | ND | ND | 1.11 |
| MP3 [e] | ND | 0.046 | ND | ND | ND | ND | ND | ND | 0.046 |
| MP4 [e] | ND | 0.39 | 0.25 | ND | ND | ND | ND | ND | 0.64 |
| MP5 [e] | ND | 1.63 | 0.60 | ND | ND | ND | ND | 0.013 | 2.24 |

[a] ND: no detection. [b] LG1–LG5, Lian-Gang industrial area. [c] MG1–MG5, municipal government. [d] MS1–MS5, monitoring station. [e] MP1–MP5, municipal party school.

**Table 4.** The predicted concentrations of PAHs in PM10 in sample set 2.

| Samples | Predicted Values (μg·mL$^{-1}$) | | | | | | | | |
|---|---|---|---|---|---|---|---|---|---|
| | **CHR** | **NAP** | **ACN** | **FLU** | **PHE** | **ANT** | **PYR** | **BaA** | **∑PAHs** |
| LG1 | ND | 3.19 | ND | ND | ND | ND | ND | ND | 3.19 |
| LG2 | ND | 1.08 | ND | ND | ND | ND | ND | ND | 1.08 |
| LG3 | ND | 4.24 | 0.10 | ND | 0.13 | ND | 0.10 | 0.022 | 4.59 |
| LG4 | ND | 7.46 | 0.79 | 0.013 | 0.48 | ND | ND | 0.007 | 8.75 |
| LG5 | ND | 3.84 | 0.16 | ND | 0.15 | ND | 0.097 | 0.023 | 4.27 |
| MS1 | ND | 7.50 | 0.085 | ND | 0.69 | ND | ND | ND | 8.28 |
| MS2 | ND | 2.13 | 0.088 | ND | 0.60 | ND | ND | ND | 2.82 |
| MS3 | ND | 5.32 | 0.17 | ND | 0.083 | ND | ND | 0.022 | 5.60 |
| MS4 | ND | 3.44 | 0.20 | ND | 0.098 | ND | ND | 0.014 | 3.75 |
| MS5 | ND | 0.33 | ND | ND | ND | ND | ND | ND | 0.33 |
| MG1 | ND | 3.10 | 0.32 | ND | 0.21 | ND | ND | ND | 3.63 |
| MG2 | ND | 1.72 | 0.14 | ND | 0.090 | ND | ND | ND | 1.95 |
| MG3 | ND | 0.36 | 0.046 | ND | ND | ND | ND | ND | 0.41 |
| MG4 | ND | 1.14 | 0.14 | ND | 0.092 | ND | ND | ND | 1.37 |
| MG5 | ND | 2.36 | 0.17 | ND | 0.14 | ND | ND | ND | 2.67 |
| MP1 | ND | 3.01 | 0.17 | ND | 0.14 | ND | ND | 0.006 | 3.33 |
| MP2 | ND | 6.33 | 0.35 | ND | 0.23 | ND | 0.13 | 0.033 | 7.07 |
| MP3 | ND | 1.63 | 0.056 | ND | ND | ND | ND | ND | 1.69 |
| MP4 | ND | 1.34 | 0.13 | ND | 0.13 | ND | ND | 0.029 | 1.63 |
| MP5 | ND | 1.92 | 0.067 | ND | 0.096 | ND | ND | ND | 2.08 |

### *4.4. Source Apportionment of PM10*

According to previous studies, the main pollution sources of PAHs in aerosols came from (1) traffic emission including BaA, CHR, ACN, and PYR [31,32], (2) home cooking producing NAP, PYR, and CHR [2,33], (3) coal combustion emitting BaA, PHE, CHR, and PYR [34], (4) waste combustion releasing PHE, FLU, and ANT [35], and (5) industrial fuel including FLU, PHE, PYR, and ANT [36]. By analysis of the component concentrations of eight PAHs in PM10 samples from different locations (Tables 3 and 4), it can be concluded

that the found PAHs in PM10 at the four sites are mainly BaA, ACN, PYR, PHE, and NAP, which most likely originated from traffic emissions and coal combustion. Figure 5A,B illustrate the results of classifying PM10 samples based on the relative concentrations of feature PAHs such as NAP, ACN, and PHE at four sites during two seasons in the city. It can be seen from the figure that PM10 samples from LG clustered together, showing clear differentiation with samples from other regions such as MG, MP, and MS, indicating that the pollution sources of PAHs in PM10 from these regions are distinct. In addition, there was a good separation of PM10 samples from Spring and Winter (see Figure 3C). Moreover, FLU, PYR, NAP, and BaA are widely distributed in aerosols sampled from industrial areas, municipal monitoring stations, and municipal party schools, indicating that the most likely sources were industrial emissions, household cooking, and coal combustion, respectively.

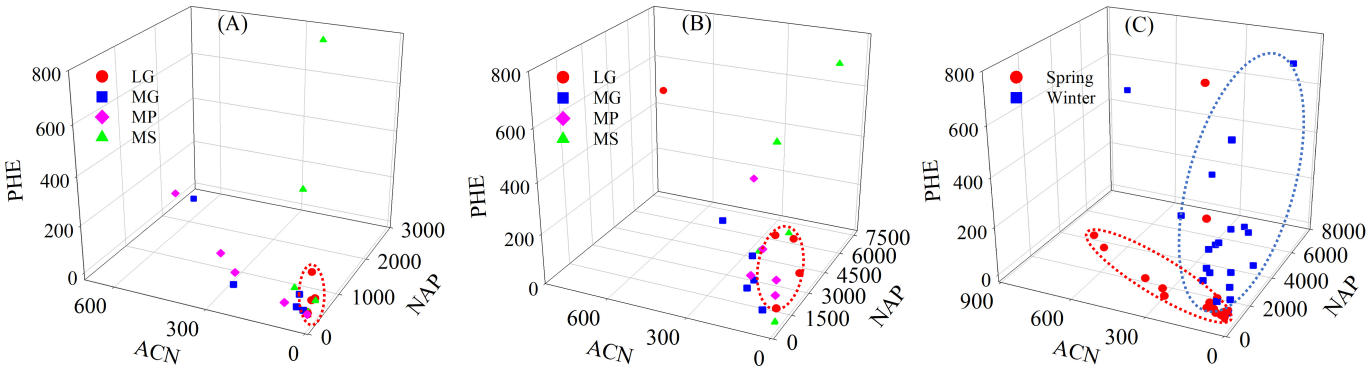


**Figure 5.** Classification of PM10 samples based on the relative concentrations of NAP vs. ACN vs. PHE at four sites in a city. (**A**) for sample set 1; (**B**) for sample set 2. (**C**) for sample sets 1 and 2. For (**A**,**B**), the cluster within the red dotted circle is mainly PM10 from LG. For (**C**), the red and blue circles for the clusters of PM10 collected during Spring and Winter, respectively.

## 5. Conclusions

The chemical composition of PM10 is very complex, with low analyte concentration and serious interference. Analysis of organic components of interest in actual PM10 has become an important and key problem in the control of toxic organic pollutants in atmospheric particulate matter. In the work, a new strategy based on the chemometric-assisted HPLC-DAD method was introduced for the rapid quantification and source apportionment of PAHs in PM10. This method capitalized on the "second-order advantage" of second-order calibration, facilitating swift and precise quantification of target components even in the presence of uncalibrated or unknown interferences. PAHs in 40 PM10 samples collected from four locations, as well as two periods in Loudi city, were rapidly quantified and source-apportioned using the developed method. Results of the feature component analysis indicated that traffic emissions and coal combustion were likely the primary sources of PAHs in the atmosphere. Additionally, with the help of second-order calibration, the proposed method eliminated the need for cumbersome pretreatment processes for complex PM10 samples, significantly shortened experimental analysis time, and reduced the use of organic solvents, fully adhering to the principles of green chemistry. In summary, the proposed method is a promising choice for the analysis of multiple PAHs in complex aerosol samples and holds substantial potential for applications in other fields such as biology, food, and medicine.

**Author Contributions:** T.H., writing—original draft, investigation, formal analysis. Y.X., writing—original draft, investigation, formal analysis. Y.W., data curation, validation. L.L., resources, project administration, writing—reviewing and editing. R.A., validation, data curation. L.X., data curation, resources, supervision, project administration. X.Q., methodology, conceptualization, writing—reviewing and editing, supervision, funding acquisition. All authors have read and agreed to the published version of the manuscript.

**Funding:** The authors gratefully acknowledge the financial support of the National Natural Science Foundation of China (Grant No. 21707032) and the Research Foundation of the Education Bureau of Hunan Province, China (Grant No. 21B0720).

**Institutional Review Board Statement:** Not applicable.

**Informed Consent Statement:** Not applicable.

**Data Availability Statement:** Data will be made available upon request.

**Conflicts of Interest:** The authors declare that they have no known competing financial interests or personal relationships that could have influenced the work reported in this paper.

## References

1. Liu, S.Z. Atmospheric PAH Contamination in the Western Watershed of Bohai Sea, China. Ph.D. Thesis, Peking University, Beijing, China, 2008.
2. Wittaya, T.; Pavidarin, K.; Somporn, C. Impact of atmospheric conditions and source identification of gaseous polycyclic aromatichydrocarbons (PAHs) during a smoke haze period in upper southeast Asia. *Toxics* **2023**, *11*, 990. [CrossRef]
3. Wang, Y.; Zhang, H.; Zhang, X.; Bai, P.C.; Zhang, L.L.; Huang, S.J.; Pointing, S.B.; Nagao, S.; Chen, B.; Toriba, A.; et al. Abundance, source apportionment and health risk assessment of polycyclic aromatic hydrocarbons and nitro-polycyclic aromatic hydrocarbons in PM2.5 in the urban atmosphere of Singapore. *Atmosphere* **2022**, *13*, 1420. [CrossRef]
4. Liao, K.Z.; Yu, J.Z. Abundance and sources of benzo[a] pyrene and other PAHs in ambient air in Hong Kong: A review of 20-year measurements (1997–2016). *Chemosphere* **2020**, *259*, 127518. [CrossRef] [PubMed]
5. Famiyeh, L.; Chen, K.; Xu, J.S.; Sun, Y.; Guo, Q.j.; Wang, C.J.; Lv, J.G.; Tang, Y.T.; Yu, H.; Snape, C.; et al. A review on analysis methods, source identification, and cancer risk evaluation of atmospheric polycyclic aromatic hydrocarbons. *Sci. Total Environ.* **2021**, *789*, 147741. [CrossRef]
6. Wu, Y.F.; Zhang, H.Q.; Zhang, H.; Zeng, T.; Qiao, N.; Shi, Y.; Zhang, N.; Luo, W.J.; Lu, S. Risks and sources of atmospheric particulate-bound polycyclic aromatic hydrocarbons (AP-PAHs) in seven regions of China: A review. *Urban Clim.* **2024**, *57*, 102108. [CrossRef]
7. Bozek, F.; Huzlik, J.; Pawelczyk, A.; Hoza, I.; Naplavova, M.; Jedlicka, J. Polycyclic aromatic hydrocarbon adsorption on selected solid particulate matter fractions. *Atmos. Environ.* **2016**, *126*, 128–135. [CrossRef]
8. Abbas, I.; Badran, G.; Verdin, A.; Ledoux, F.; Roumié, M.; Courcot, D.; Garçon, G. Polycyclic aromatic hydrocarbon derivatives in airborne particulate matter: Sources, analysis and toxicity. *Environ. Chem. Lett.* **2018**, *16*, 439–475. [CrossRef]
9. Krzyszczak, A.; Czech, B. Occurrence and toxicity of polycyclic aromatic hydrocarbons derivatives in environmental matrices. *Sci. Total Environ.* **2021**, *788*, 147738. [CrossRef]
10. Vosough, M. Current challenges in second-order calibration of hyphenated chromatographic data for analysis of highly complex samples. *J. Chemom.* **2018**, *32*, e2976. [CrossRef]
11. Dogra, R.; Kumar, M.; Kumar, A.; Roverso, M.; Bogialli, S.; Pastore, P.; Mandal, U.K. Derivatization, an applicable asset for conventional HPLC systems without MS detection in food and miscellaneous analysis. *Crit. Rev. Anal. Chem.* **2023**, *53*, 1807–1827. [CrossRef]
12. Santanatoglia, A.; Angeloni, S.; Fiorito, M.; Fioretti, L.; Ricciutelli, M.; Sagratini, G.; Vittori, S.; Caprioli, G. Development of new analytical methods for the quantification of organic acids, chlorogenic acids and caffeine in espresso coffee by using solid-phase extraction (SPE) and high-performance liquid chromatography-diode array detector (HPLC-DAD). *J. Food Compos. Anal.* **2024**, *125*, 105732. [CrossRef]
13. Lovato, G.; Ciriolo, L.; Perrucci, M.; Federici, L.; Ippoliti, R.; Iacobelli, S.; Capone, E.; Locatelli, M.; Sala, G. HPLC-DAD validated method for DM4 and its metabolite S-Me-DM4 quantification in biological matrix for clinical and pharmaceutical applications. *J. Pharm. Biomed. Anal.* **2023**, *235*, 115642. [CrossRef] [PubMed]
14. Świt, P.; Orzeł, J.; Maślanka, S. Monitoring of PAHs in simulated natural and artificial fires by HPLC-DAD-FLD with the application of Multi-Component Integrated calibration method to improve quality of analytical results. *Measurement* **2022**, *196*, 111242. [CrossRef]
15. Escandar, G.M.; de la Peña, A.M. Multi-way calibration for the quantification of polycyclic aromatic hydrocarbons in samples of environmental impact. *Microchem. J.* **2021**, *164*, 106016. [CrossRef]
16. Qing, X.D.; Wu, H.L.; Zhang, X.H.; Li, Y.; Gu, H.W.; Yu, R.Q. A novel fourth-order calibration method based on alternating quinquelinear decomposition algorithm for processing high performance liquid chromatography-diode array detection-kinetic-pH data of naptalam hydrolysis. *Anal. Chim. Acta* **2015**, *861*, 12–24. [CrossRef] [PubMed]
17. Qing, X.D.; Wu, H.L.; Zhang, X.H.; Li, Y.; Gu, H.W.; Wen, J.; Shen, X.Z.; Yu, R.Q. A new alternating weighted quadrilinear decomposition algorithm with application for analysis of non-quinquelinear five-way data arrays. *Sci. Sin. Chim.* **2016**, *46*, 401–408. [CrossRef]
18. Chiappini, F.A.; Alcaraz, M.R.; Escandar, G.M.; Goicoechea, H.C.; Olivieri, A.C. Chromatographic applications in the multi-way calibration field. *Molecules* **2021**, *26*, 6357. [CrossRef]

19. Wu, H.L.; Long, W.J.; Wang, T.; Dong, M.Y.; Yu, R.Q. Recent applications of multiway calibration methods in environmental analytical chemistry: A review. *Microchem. J.* **2020**, *159*, 105575. [CrossRef]
20. Qing, X.D.; Zhang, X.H.; An, R.; Zhang, J.; Xu, L.; Duponchel, L. A fast and robust third-order multivariate calibration approach coupled with excitation-emission matrix phosphorescence for the quantification and oxidation kinetic study of fluorene in wastewater samples. *Chemosensors* **2023**, *11*, 53. [CrossRef]
21. Wells, M.J.; Funk, D.; Mullins, G.A.; Bell, K.Y. Application of a fluorescence EEM-PARAFAC model for direct and indirect potable water reuse monitoring: Multi-stage oarea-biofiltration without reverse osmosis at Gwinnett County, Georgia, USA. *Sci. Total Environ.* **2023**, *886*, 163937. [CrossRef]
22. Cavaglia, J.; Garcia, S.M.; Roger, J.; Mestres, M.; Boqué, R. Detection of bacterial spoilage during wine alcoholic fermentation using ATR-MIR and MCR-ALS. *Food Control* **2022**, *142*, 109269. [CrossRef]
23. Wu, H.L.; Shibukawa, M.; Oguma, K. An alternating trilinear decomposition algorithm with application to calibration of HPLC-DAD for simultaneous determination of overlapped chlorinated aromatic hydrocarbons. *J. Chemom.* **1998**, *12*, 1–26. [CrossRef]
24. Yu, J.; Zhang, X.Y.; Hou, D.B.; Chen, F.; Mao, T.T.; Huang, P.J.; Zhang, G.X. Detection of water contamination events using fluorescence spectroscopy and alternating trilinear decomposition algorithm. *J. Spectrosc.* **2017**, *1*, 1485048. [CrossRef]
25. Tan, F.Y.; Tan, C.; Zhao, A.P.; Li, M.L. Simultaneous determination of free amino acid content in tea infusions by using high-performance liquid chromatography with fluorescence detection coupled with alternating penalty trilinear decomposition algorithm. *J. Agric. Food Chem.* **2011**, *59*, 10839–10847. [CrossRef] [PubMed]
26. Yan, L.; Qian, W.; Xia, Z.Z.; Wu, Y.; Li, Y.; Gong, Z.Y. Simultaneous and rapid determination of sesamin and sesamolin in sesame oils using excitation-emission matrix fluorescence coupled with self-weighted alternating trilinear decomposition. *J. Sci. Food Agric.* **2020**, *100*, 4418–4424. [CrossRef]
27. Zhang, X.H.; Qing, X.D.; Zhang, J.J.; Yu, Y.; Huang, J.; Kang, C.; Liu, Z. Aqueous two-phase systems coupled with chemometrics-enhanced HPLC-DAD for simultaneous extraction and determination of flavonoids in honey. *Food Chem. X* **2023**, *19*, 100766. [CrossRef]
28. Valverde-Som, L.; Reguera, C.; Herrero, A.; Sarabia, L.A.; Ortiz, M.C. Determination of polymer additive residues that migrate from coffee capsules by means of stir bar sorptive extraction-gas chromatography-mass spectrometry and PARAFAC decomposition. *Food Packag. Shelf Life* **2021**, *28*, 100664. [CrossRef]
29. Chen, Y.; Wu, H.L.; Wang, T.; Sun, X.D.; Liu, B.B.; Chang, Y.Y.; Chen, J.C.; Ding, Y.J.; Yu, R.Q. Quantitative analysis of carbaryl and thiabendazole in complex matrices using excitation-emission fluorescence matrices with second-order calibration methods. *Spectrochim. Acta A* **2021**, *264*, 120267. [CrossRef]
30. Rasmus, B.; Henk, A.L. A new efficient method for determining the number of components in PARAFAC models. *J. Chemom.* **2003**, *17*, 274–286. [CrossRef]
31. Xing, W.L.; Yang, L.; Zhang, H.; Zhang, X.; Wang, Y.; Bai, P.C.; Zhang, L.L.; Hayakawa, K.; Nagao, S.; Tang, N. Variations in traffic-related polycyclic aromatic hydrocarbons in PM2.5 in Kanazawa, Japan, after the implementation of a new vehicle emission regulation. *J. Environ. Sci.* **2022**, *121*, 38–47. [CrossRef]
32. Najmeddin, A.; Keshavarzi, B. Health risk assessment and source apportionment of polycyclic aromatic hydrocarbons associated with PM10 and road deposited dust in Ahvaz metropolis of Iran. *Environ. Geochem. Health* **2019**, *41*, 1267–1290. [CrossRef] [PubMed]
33. Wu, F.Y.; Liu, X.P.; Wang, W.; Man, Y.B.; Chan, C.Y.; Liu, W.X.; Tao, S.; Wong, M.H. Characterization of particulate-bound PAHs in rural households using different types of domestic energy in Henan Province, China. *Sci. Total Environ.* **2015**, *536*, 840–846. [CrossRef] [PubMed]
34. Giandomenico, S.; Nigro, M.; Parlapiano, I.; Spada, L.; Grattagliano, A.; Prato, E.; Biandolino, F. Effect of in-house cooking in Mytilus galloprovincialis and Trachurus trachurus: Lipid and fatty acids quality and polycyclic aromatic hydrocarbons formation. *Food Chem. Toxicol.* **2023**, *173*, 113606. [CrossRef] [PubMed]
35. Fakinle, B.S.; Odekanle, E.L.; Ike-Ojukwu, C.; Sonibare, O.O.; Falowo, O.A.; Olubiyo, F.W.; Oke, D.O.; Aremu, C.O. Quantification and health impact assessment of polycyclic aromatic hydrocarbons (PAHs) emissions from crop residue combustion. *Heliyon* **2022**, *8*, e09113. [CrossRef]
36. Forcada, S.; Menéndez, M.M.; Stevens, F.; Royo, L.J.; Pierna, J.A.F.; Baeten, V.; Soldado, A. Industrial impact on sustainable dairy farms: Essential elements, hazardous metals and polycyclic aromatic hydrocarbons in forage and cow's milk. *Heliyon* **2023**, *9*, e20977. [CrossRef]


**Disclaimer/Publisher's Note:** The statements, opinions and data contained in all publications are solely those of the individual author(s) and contributor(s) and not of MDPI and/or the editor(s). MDPI and/or the editor(s) disclaim responsibility for any injury to people or property resulting from any ideas, methods, instructions or products referred to in the content.